

**ENGINEERING DEVELOPMENT OF SLURRY BUBBLE COLUMN REACTOR
(SBCR) TECHNOLOGY**

Quarterly Technical Progress Report No. 17

For the Period 1 April – 30 June 1999

FINAL

Contractor
AIR PRODUCTS AND CHEMICALS, INC.
7201 Hamilton Blvd.
Allentown, PA 18195-1501

Bernard A. Toseland, Ph.D.
Program Manager and Principal Investigator

Robert M. Kornosky
Contracting Officer's Representative

Prepared for the United States Department of Energy
Under Cooperative Agreement No. DE-FC22-95PC95051
Contract Period 3 April 1995 – 2 April 2000

**NOTE: AIR PRODUCTS DOES NOT CONSIDER ANYTHING IN THIS
REPORT TO BE CONFIDENTIAL OR PATENTABLE.**

ENGINEERING DEVELOPMENT OF SLURRY BUBBLE COLUMN REACTOR (SBCR) TECHNOLOGY

Quarterly Technical Progress Report No. 17 For the Period 1 April – 30 June 1999

Contract Objectives

The major technical objectives of this program are threefold: 1) to develop the design tools and a fundamental understanding of the fluid dynamics of a slurry bubble column reactor to maximize reactor productivity, 2) to develop the mathematical reactor design models and gain an understanding of the hydrodynamic fundamentals under industrially relevant process conditions, and 3) to develop an understanding of the hydrodynamics and their interaction with the chemistries occurring in the bubble column reactor. Successful completion of these objectives will permit more efficient usage of the reactor column and tighter design criteria, increase overall reactor efficiency, and ensure a design that leads to stable reactor behavior when scaling up to large diameter reactors.

WASHINGTON UNIVERSITY IN ST. LOUIS

The report from Washington University for the period follows.

ENGINEERING DEVELOPMENT OF SLURRY BUBBLE COLUMN REACTOR (SBCR) TECHNOLOGY

**Seventeenth Quarterly Report
for
1 April – 30 June 1999**

(Budget Year 4: 1 October 1998 – 30 September 1999)

Objectives for the Fourth Budget Year

The main goal of this subcontract from the Department of Energy via Air Products to the Chemical Reaction Engineering Laboratory (CREL) at Washington University is to study the fluid dynamics of slurry bubble columns and address issues related to scaleup and design. The objectives set for the fourth budget year (1 October 1998 – 30 September 1999) are listed below:

- Extension of CARPT/CT database to conditions of industrial interest such as high superficial gas velocity (up to 30-50 cm/s).
- Examination of the improved gas mixing phenomenological model against LaPorte tracer data.
- Critical evaluation of the developed phenomenological models for liquid and gas mixing against the newly obtained data.
- Testing of the 4-points optical probe for bubble size and bubble rise velocity measurements.
- Further improvement in Computational Fluid Dynamics (CFD) using CFDLIB and FLUENT through development of improved closure schemes and comparison of 2D and 3D model predictions with 2D and 3D data.

In this report, the research progress and achievements accomplished in the seventeenth quarter (April 1 - June 30, 1999) are summarized.

HIGHLIGHTS

Characterization of Gas Phase Mixing Via Gas-Liquid Recirculation Model (GLRM)

- A completely implicit finite difference scheme has been developed for the simulation of coupled partial and ordinary differential equations with Danckwert's boundary conditions, which describe the two-bubble class gas-liquid recirculation model.
- The radioactive gas tracer experiments have been simulated using the developed two-bubble class gas-liquid recirculation model. The model was used strictly in the predictive sense, with all the parameters estimated independently and not by the fitting of tracer data.
- The model predicts the tracer to be leaving the system faster than the experimentally observed tracer responses. This points out the importance of the precise knowledge of the radial gas holdup profile, since it is this profile that determines the rate of gas and liquid recirculation, and therefore, the average speed of tracer propagation.

Simulation of Gas-Liquid Flow in Cylindrical Bubble Columns with FLUENT: Comparison with CARPT-CT Experimental Results

- Three-dimensional (3D) simulation was performed using two different modeling approaches: the two-fluid Euler-Euler approach and the algebraic slip mixture model approach.
- The simulation was performed for a gas superficial velocity of 12.0 cm/s at atmospheric pressure, typical of churn-turbulent flow regime.
- Reasonably good agreement was obtained between simulated and experimentally determined, time-averaged, axial liquid velocity profiles (measured via CARPT) and time-averaged gas holdup profiles (measured via CT).

1. CHARACTERIZATION OF GAS PHASE MIXING VIA GAS-LIQUID RECIRCULATION MODEL (GLRM)

In the monthly reports for January and February 1999 and in the 16th quarterly report, the detailed model development of a two-bubble-class, gas-liquid recirculation model was presented to characterize mixing in both the gas and liquid phases. A one-dimensional (1D) sub-model based on the two-fluid concept was also presented to compute the 1D

radial profiles of the time-averaged liquid and gas axial velocities. These velocity profiles were then appropriately averaged to obtain the various parameters in the two-bubble-class, gas-liquid recirculation model, as outlined in the monthly report for February 1999 and in the 16th quarterly report. In this report, we present the solution methodology for the model equations, along with the simulation results for radioactive gas tracer runs executed at the LaPorte Alternate Fuels Development Unit during methanol synthesis.

1.1 Two-Bubble Class Gas-Liquid Recirculation Model

The model equations to be simulated and the associated boundary conditions for the PDEs have been detailed in the 16th quarterly report. The initial conditions for the tracer inlet to be used for simulation of the model equations depends on the method of tracer injection, and on whether it is an impulse tracer test or a step-up/step-down tracer test. The experimental impulse input for the tracer runs at LaPorte have been simulated using a Gaussian function with a tail (Degaleesan, 1997).

$$t \rightarrow 0^+, t > 0; C_{g,in} = \frac{\psi}{\sqrt{2\pi\kappa t}} \exp\left\{-\frac{(\delta-\chi)^2}{2\kappa t}\right\} \quad (1.1)$$

The parameters in the simulated gas tracer injection profile for the different tracer runs are listed in Table 1.1.

1.2 Solution Procedure

The system of coupled partial differential equations (PDEs) and ordinary differential equations (ODEs) is solved using a completely time-implicit finite difference procedure; the time derivatives are approximated with first-order accurate forward differences. The spatial derivatives are discretized using second-order accurate central differences evaluated at the (n+1) time level to make the scheme completely implicit. Since for the tracer simulation, the liquid phase reaction terms, which could have a non-linear form, are absent, the resulting set of equations is linear, and one can resort to direct inversion of the solution matrix. Even though direct matrix inversion is computationally expensive, for the linear problem at hand, it does not pose any problems, since the inverse needs to be evaluated only once. Subsequently, the solution at successive time levels is obtained by simple matrix multiplication. In this work, this solution has been accomplished using LU (lower/upper) decomposition followed by repetitive LU back-substitution.

1.3 Results

Figures 1.1, 1.2 and 1.3 show the comparison of the model predictions with the experimental gas tracer responses from Runs 14.6, 14.7 and 14.8 during methanol synthesis at the LaPorte AFDU. The three detector levels along the reactor vertical axis at which the comparisons are made are shown in Figure 1.4. In the legend in Figures 1.1, 1.2

and 1.3 “Exp” refers to experimental data, whereas “Sim” refers to model predictions. L1, L4 and L7 refer to the three detector levels (Figure 1.4) at which comparisons have been made.

As shown in Figure 1.1 for Run 14.6 ($U_g=25$ cm/s and $P=5.2$ MPa), the prediction of the tracer responses is quite promising, as no fitting parameters have been used in the model simulation. On the other hand, in Figure 1.2 for Run 14.7, in which the gas superficial velocity was 14.3 cm/s and the operating pressure was 5.2 MPa, the predicted tracer responses are significantly leading the experimentally obtained responses. This implies that the velocity profiles of the gas and liquid/slurry, predicted by the sub-models during tracer response simulation, are much higher than the actual gas and liquid recirculation rates. Moreover, experimental tracer curves indicate that gas holdup may be higher than estimated. However, for Run 14.8, in which the gas superficial velocity was much higher at 36 cm/s with a lower system pressure of 3.6 MPa, the model predictions again appear to be in better agreement with the experimental data, as shown in Figure 1.3.

1.4 Discussion and Future Work

The comparison of the simulated tracer responses to those obtained experimentally are strictly the outcome of a systematic attempt to tie fundamentals to experimental observations; no attempt has been made to fit the predicted and experimentally observed curves by arbitrary choice of the various parameters required in the solution of the model equations. The results from the Axial Dispersion Model (ADM) for these tracer experiments were analyzed in an independent report (Degaleesan *et al.*, 1996). In that study, the tracer responses were matched to experimental data at various elevations by curve fitting. To achieve acceptable fits, the values of two or three parameters, such as the average gas holdup, $\epsilon_{g,avg}$, the effective dispersion coefficient of the gas phase, D_g , the volumetric mass transfer coefficient, $k_L a$, and the Henry's constant, H , were adjusted. However, no consistent trends were found, as reported, in the estimated parameter values for any of the experimental tracer runs. In addition, the liquid phase dispersion coefficients, required for the solution of the gas phase tracer equations, were taken to be those obtained from the fits of the liquid tracer data by ADM. It was also reported that the model predictions were very sensitive to the Henry's constant and were considerably less affected by the other model parameters. In light of these observations, the model predictions from the two-bubble class gas-liquid recirculation model are promising, since no fitting parameters have been used so far in the model simulations.

The following issues related to the improvement of the model predictions still remain to be addressed:

- In the simulation of the liquid and gas velocity profiles, a radial gas holdup profile proposed by Kumar (1994) was used as input. Such a profile has three parameters, the average gas holdup, $\epsilon_{g,avg}$, the exponent, m , indicating the nature of the radial dependence of holdup (e.g., the lower the m the steeper the holdup profile) and a parameter, c , related to the gas holdup close to the wall (the lower the c the higher

the wall holdup). To determine these parameters uniquely from experimental data, one needs to have either a CT scan of the holdup distribution or three independent measurements of say chordal and cross-sectional average holdup and holdup at the wall. For the tracer runs at hand, only two independent measurements were available, i.e., chordal average via Nuclear Gauge Densitometry (NDG) and cross-sectional average via pressure drop. Thus, one could not extract a unique gas holdup profile from the measurements. To circumvent this problem, the value of the exponent m was fixed at 2, since the superficial gas velocities were all in excess of 10-12 cm/s, and one would expect the column to operate under churn-turbulent conditions. However, the assumption of m being 2 might not be as appropriate as originally thought based on our recent experience with a laboratory-scale, high-pressure bubble column operated at pressures up to 10 atm; in that column, values of m in the range of 2.9-3.5 were observed, even at higher gas superficial velocity. This indicates that increased system pressure results in a flatter radial gas holdup profile, thereby reducing the rates of liquid circulation and subsequently of the gas recirculation. Since the AFDU is operated at pressures exceeding the highest operating pressure of our laboratory unit, the use of $m = 2$ becomes questionable. Therefore, a sensitivity analysis of the effect of radial gas profile on the simulated responses is being carried out, and the results will be reported in the future.

- The second issue that needs to be addressed is the sensitivity of the model predictions to the Henry's constant. From a preliminary analysis, the results appear to be quite sensitive, and a systematic analysis is being made to assess the bounds on the range of the possible values for the Henry's constant.
- The third issue that remains to be addressed is the distribution of the gas phase between small and large bubbles. Currently, the methodology of Krishna and Ellenberger (1996) is being used to estimate the relative holdups of the large and small bubbles, as well as the bubble sizes. The sensitivity to these parameters needs to be investigated. In light of this need, a single-bubble class model is also being developed that does not suffer from the arbitrariness of the assignment of the relative holdups of the large and small bubbles. It remains to be seen whether a single-bubble class model can provide predictions in better agreement with the experimental data.

1.5 References

Degaleesan, S., "Fluid dynamic measurements and modeling of liquid mixing in bubble columns," *D.Sc. Thesis*, Washington University (1997).

Degaleesan, S., M. P. Dudukovic', B. L. Bhatt, and B. A. Toseland, "Slurry bubble column hydrodynamics: tracer studies of the LaPorte AFDU reactor during methanol synthesis," *Fourth Quarterly Report for Contract DOE-FC 2295 PC 95051* (1996).

Krishna, R., and J. Ellenberger, "Gas holdup in bubble column reactors operating in the churn-turbulent flow regime," *AIChE J.*, **42** (9), 2627 (1996).

Kumar, S. B., "Computed tomographic measurements of void fraction and modeling of the flow in bubble columns," *Ph.D. Thesis*, Florida Atlantic University (1994).

Table 1.1 Parameters in the Expression for the Simulated Tracer Input for Different Tracer Runs

Run	ψ	κ	δ	χ
14.6	71.9	600	40	25.3
14.7	39.5	250	18	14.3
14.8	104.0	1500	50	36.0

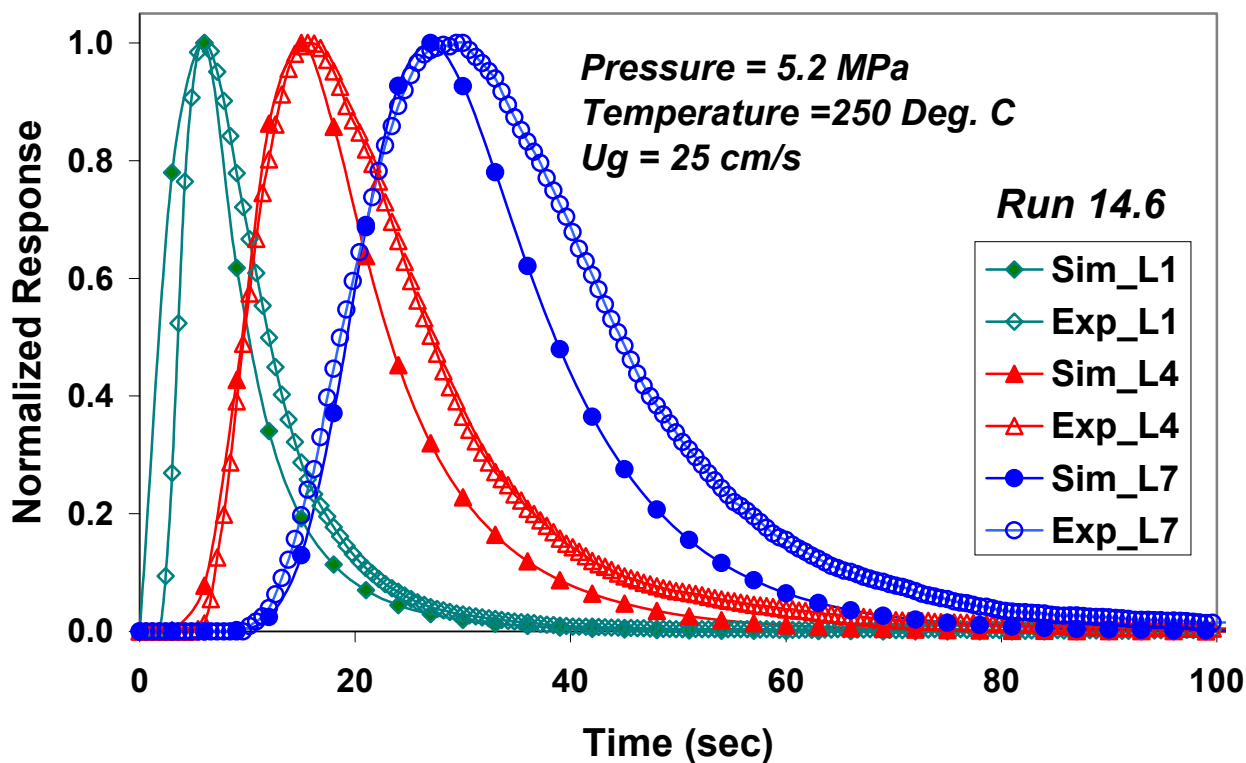


Figure 1.1 Schematic Representation of the Experimentally Observed Phenomena in Bubble Columns

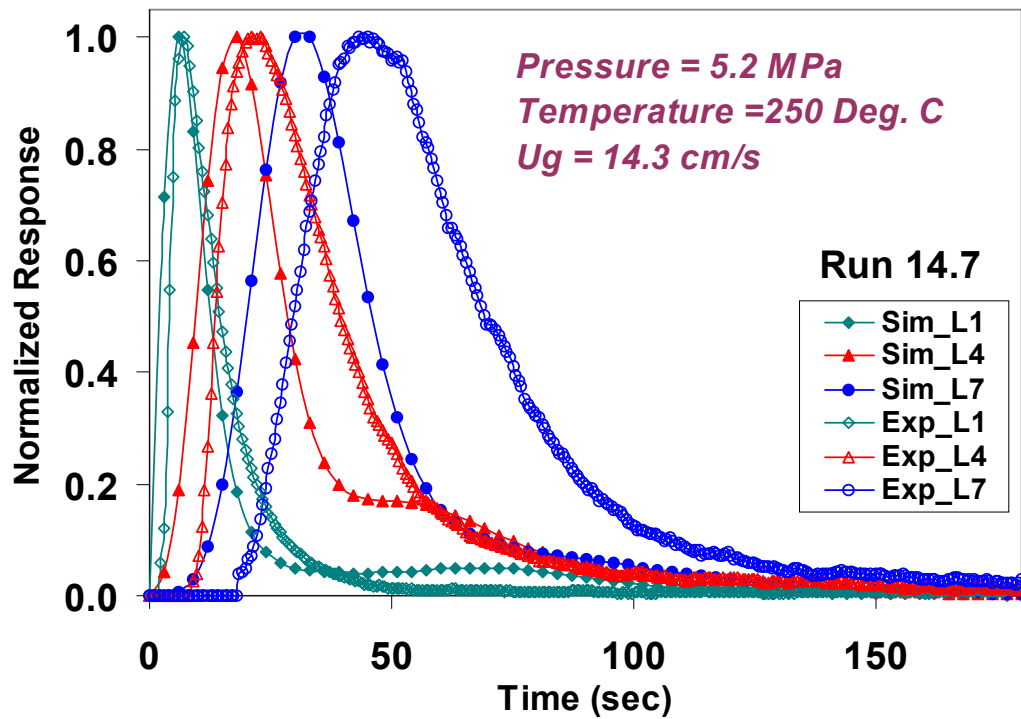


Figure 1.2 Comparison of Simulated and Experimental Tracer Responses for Run 14.7

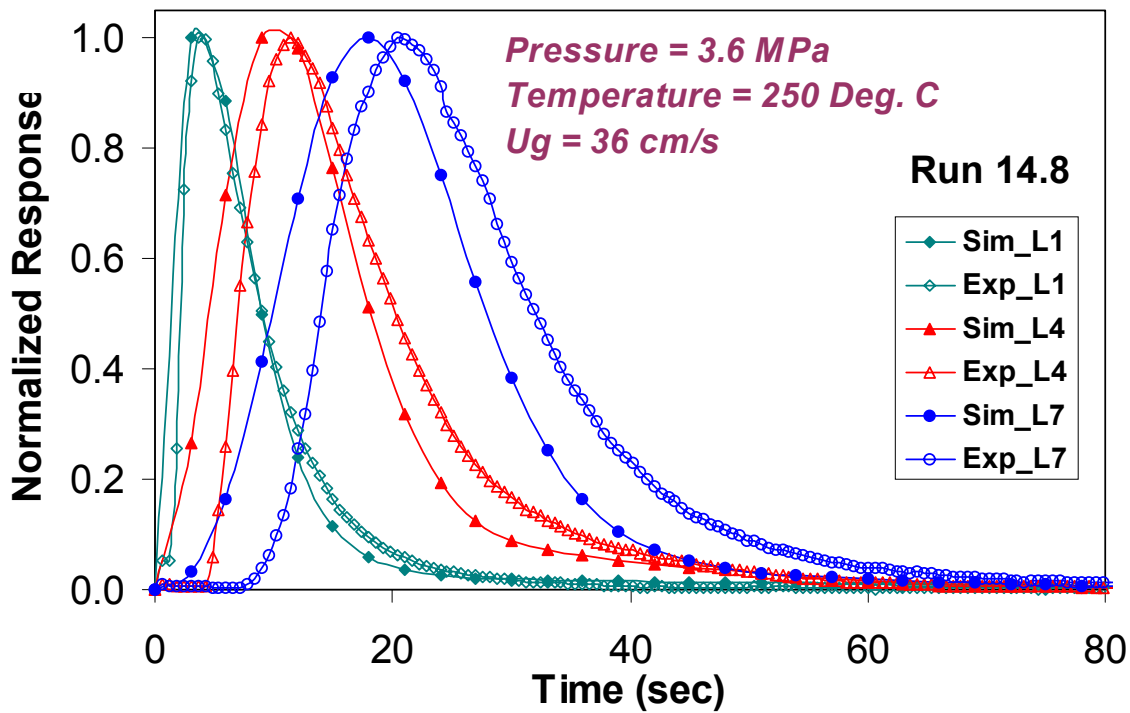


Figure 1.3 Comparison of Simulated and Experimental Tracer Responses for Run 14.8

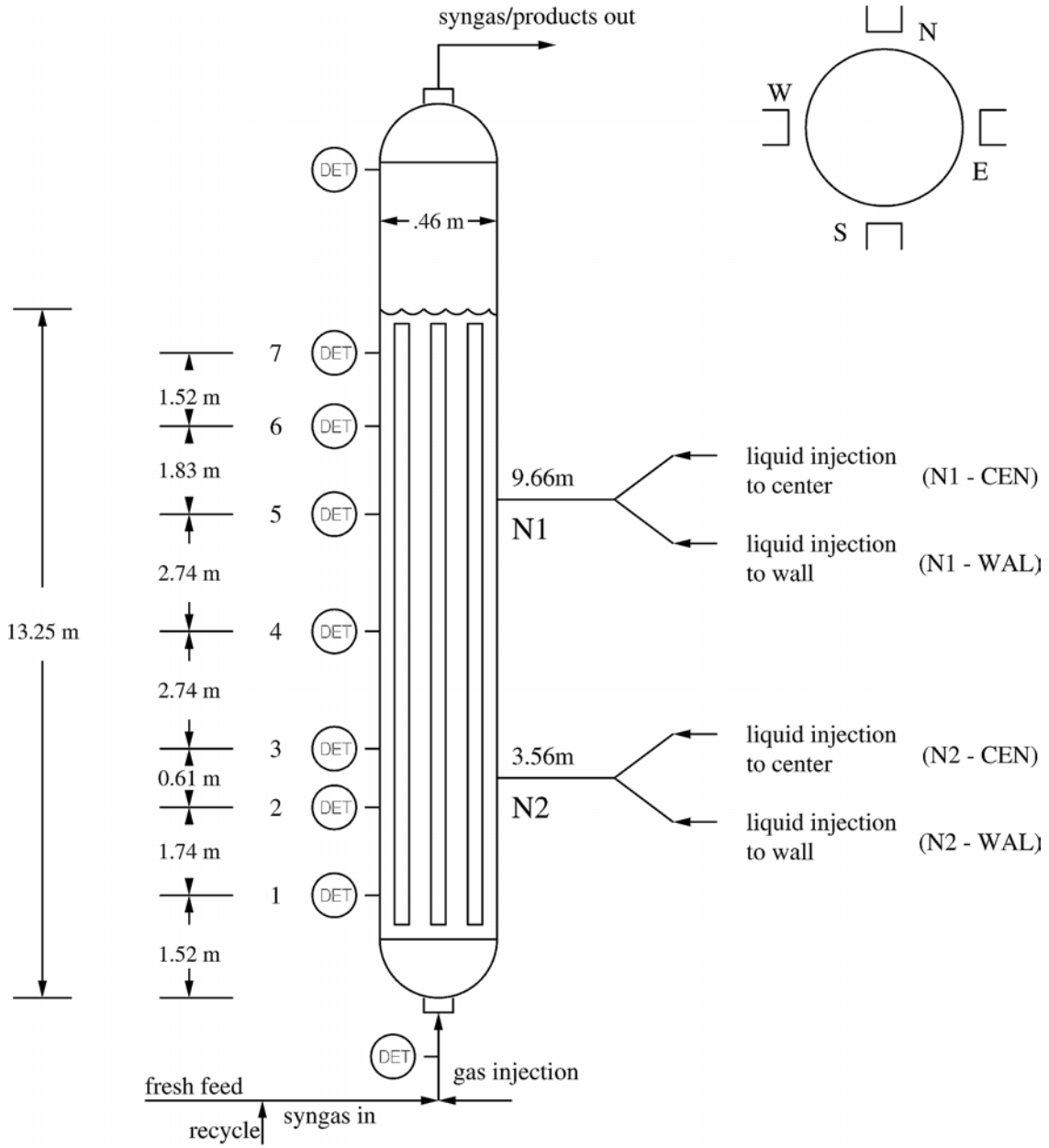


Figure 1.4 Schematic Representation of the LaPorte AFDU Indicating the Detector Levels

2. SIMULATION OF GAS-LIQUID FLOW IN CYLINDRICAL BUBBLE COLUMNS WITH FLUENT: COMPARISON WITH CARPT-CT EXPERIMENTAL RESULTS

Validation of a transient, three-dimensional simulation of a laboratory-scale cylindrical bubble column was attempted using the experimental data collected with CARPT and CT techniques in our laboratory under operating conditions identical to those employed in the simulation. The numerical simulation was effected using the FLUENT library of codes.

This report presents the investigation, which follows our earlier work on two-dimensional axisymmetric modeling of two-phase flow in bubble columns (Monthly Report, December, 1998; 15th quarterly report). There we had observed that while the agreement between simulation predictions and experimental data for time-averaged axial liquid velocity was reasonably good, the comparison for gas holdup was not (although the correct trends could be captured). Since in reality the flow in bubble columns is not axisymmetric, with significant azimuthal components of velocity, we were motivated to perform full three-dimensional simulations to capture those effects, as well as obtain better comparison for time-averaged flow quantities. Some initial results of this investigation are presented here.

This series of investigations attempts to build a framework for three-dimensional simulations coupled with heat transfer, mass transfer, volatility effects and chemical reactions. Such efforts will lead us to using computational fluid dynamics (CFD) techniques for simulating larger scale pilot plant and industrial bubble columns, and hopefully serve as design and scaleup tools in the future.

2.1 Results and Discussion:

2.1.1 Two-Fluid Euler-Euler Model (TFEEM):

In the Eulerian two-fluid approach (Anderson and Jackson, 1967), the two phases (gas and liquid) are treated as interpenetrating continua, and the probability of occurrence of any one phase in multiple realizations of the flow is given by the instantaneous volume fraction of that phase at that point. The sum total of all volume fractions at a point is identically unity. Both fluids are treated as incompressible, and a single pressure field is shared by all phases. Continuity and momentum equations are solved for each phase. Momentum transfer between the phases is modeled through a drag term, which is a function of the local slip velocity between the phases. A characteristic diameter is assigned to the gas bubbles of the dispersed phase, and a drag formulation based on a single sphere settling in an infinite medium is used (Morsi and Alexander, 1972). Turbulence in either phase is modeled separately using the standard k - ϵ model, modified with terms accounting for two-phase flow (Elghobashi and Abou-Arab, 1983).

2.1.2 Algebraic Slip Mixture Model (ASMM):

The ASMM (Manninen *et al.*, 1996) also models the phases as two interpenetrating continua, with the probability of existence of each phase at a point in the computational

domain given by its respective volume fraction (holdup). In general, the two phases move at different velocities. However, in contrast to the two-fluid Euler-Euler approach, a *separate* equation is solved for the continuity and for the momentum of the *mixture*. Motion of each phase relative to the center of mass of the mixture in any control volume is viewed as a diffusion of that phase; this introduces the concept of a diffusion velocity of each phase. Since the equations are solved for the mixture, no formulation for *drag* (which models momentum transfer *between* the phases) is required.

The Reynolds' averaged mixture momentum equation has a term, called *diffusion stress*, that originates because of the relative slip between the two phases. This requires closure in terms of the diffusion velocity of each phase (or, equivalently, the drift or the slip velocity between the phases). In the ASMM, this is supplied by assuming that the phases are in *local equilibrium over short spatial length scales*. This means that the dispersed phase entity (bubble, particle) always slips with respect to the continuous phase at its terminal Stokes' velocity in the local acceleration field.

The *diffusion stress* term is also the only term in which the phase volume fractions appear explicitly. In order to back out the individual phase velocities and volume fraction at the end of the computation at each time step, it is necessary to solve a differential equation for the volume fraction of the dispersed phase, coupled with the solution of the mixture equations. This equation is obtained from the equation of continuity for the dispersed phase. Finally, the turbulent stress term in the mixture equation is closed by solving a k - ϵ model for the *mixture* phase.

A detailed description and the equations used for either model have been presented in our 15th quarterly report. In the present simulations, only the dimensionality of the problem (i.e., three dimensions) is different.

2.1.3 Simulation Predictions

A full three-dimensional simulation of the 19-cm diameter bubble column, operating in churn-turbulent flow at a gas superficial velocity of 12 cm/s, was implemented in FLUENT. The parameters used in the simulation are shown in Table 2.1.

In Figure 2.1, liquid velocity vector plots are presented at a given time, 10.04 s after the inflow of gas into the column was started. The velocity vectors are colored by gas volume fraction, red being a high-volume fraction of gas and blue being a low-volume fraction. Figure 2.1(a) shows the vectors in a vertical plane, while Figures 2.1(b), 2.1(c) and 2.1(d) display the vectors in three horizontal planes. The swirling motion in the liquid phase is clearly observable, with higher magnitude of liquid velocity (longer vectors) in the regions of high gas volume fraction (red) (because the liquid is “driven” by the gas rising due to the buoyancy difference). In Figure 2.2, the gas volume fraction contours are shown at a horizontal plane roughly half-way up the column (i.e., at a height of 66.6 cm) at four different time instants. The transient character of the gas volume fraction, due to rapidly oscillating bubble plumes, is highlighted in these plots.

The time-averaged flow profiles from these transient results can be readily compared against the time-averaged data from the CARPT and CT experiments. The comparisons are presented in Figures 2.3 and 2.4 for time-averaged axial liquid velocity and gas volume fraction, respectively. The simulation was allowed to reach stationary state in 40 s (i.e., the gas-liquid interface motion became invariant with time), following which the averaging was done for an additional 40 s. The time-averaged quantities presented in Figures 2.3 and 2.4 were invariant with time for calculation periods of more than 30 s (i.e., 40 s is sufficient averaging time for the simulated conditions). The comparison of the time-averaged liquid velocity calculated by the model and obtained from the CARPT experiment (Figure 2.3) indicated very good agreement. The centerline liquid velocity, the cross-over point and the maximum downflow liquid velocity were all predicted with good fidelity. Predictions of the two models (i.e., two-fluid and ASMM) were also comparable. However, for the gas volume fraction, the models underpredicted the time-averaged CT data somewhat, although the predictions were much better than what was observed with a 2D axisymmetric simulation (Monthly Report, December 1998; 15th quarterly report). Thus, relaxing the assumption of axisymmetry and performing a full 3D simulation definitely improves the results. The computation times for the same set of flow conditions were much higher for the 3D simulation, and also much more virtual memory and hard disk space were required. Thus, for engineering approximations and order-of-magnitude estimates of the flow quantities, the assumption of 2D axisymmetry may be sufficient. For more detailed simulations, a full three-dimensional simulation should be performed. The improvement of the predictions with the 3D simulation may prove to be more dramatic when heat transfer, mass transfer and reactions are coupled with the fluid motion.

In spite of the improvement observed with the 3D simulation, it is clear that better prediction of gas holdup is required. This may be sought by either of the following means:

- use of an improved drag correlation, which models the momentum transfer from gas to liquid phase in bubble swarms (clearly, currently lesser gas holdup seems to drive more liquid flow in the simulation when compared to the real experiment).
- use of a "better" closure form for turbulence, such as one for bubble-induced turbulence, because closures like the k - ϵ model account only for shear-induced turbulence.

Work on the above approaches will be performed in subsequent months. In parallel, modeling of transport of an inert liquid-phase tracer is being investigated, as this is the first step for extending the present models for prediction of reactant conversion and product selectivity in reaction systems.

2.2 References

- Anderson, T. B. and R. Jackson, "A fluid dynamical description of fluidized beds," *Ind. Engng. Chem. Fund.* 6, 527-534 (1967).
- Degaleesan, S., "Fluid dynamic measurements and modeling of liquid mixing in bubble columns," *D. Sc. Thesis*, Washington University in St. Louis, Missouri, USA (1997).
- Elgobashi, S. E. and T. W. Abou-Arab, "A two-equation turbulence model for two-phase flows," *Phys. Fluids* 26(4), 931-938 (1983).
- Morsi, S. A. and A. J. Alexander, "An investigation of particle trajectories in two-phase flow systems," *J. Fluid Mech.* 55(2), 193-208 (1972).
- Manninen, M., V. Taivassalo, and S. Kallio, "On the mixture model for multiphase flow," VIT Publications, Technical Research Center of Finland (1996).
- Wallis, G. "One-dimensional two-phase flow," McGraw-Hill, New York, USA (1969).
- DOE Reports:*
- Monthly Report for December 1998: "Simulation of gas-liquid flow in cylindrical bubble columns with FLUENT: comparison with CARPT-CT experimental results."
- 15th Quarterly Report, October-December, 1998.

Table 2.1 Parameters Used in the Three-Dimensional Simulation

Grid	200 (axial) × 19 (radial) × 36 (radial)
Cell Size	0.66 cm (axial) × 0.5 cm (radial) × 10 ⁰ (radial) (uniform grid)
Time Step	0.01 s (Euler-Euler); 0.005 s (ASMM)
Iterations per Time Step for Convergence	around 25
Under-Relaxation Parameters	Euler-Euler: 0.6 (pressure), 0.4 (velocities); ASMM: 0.3 (pressure), 0.7 (velocities).
Bubble Size	0.5 cm
Drag Formulation	Single Sphere Drag Correlation (Morsi and Alexander, 1972)
Turbulence Model	Standard k - ϵ Model

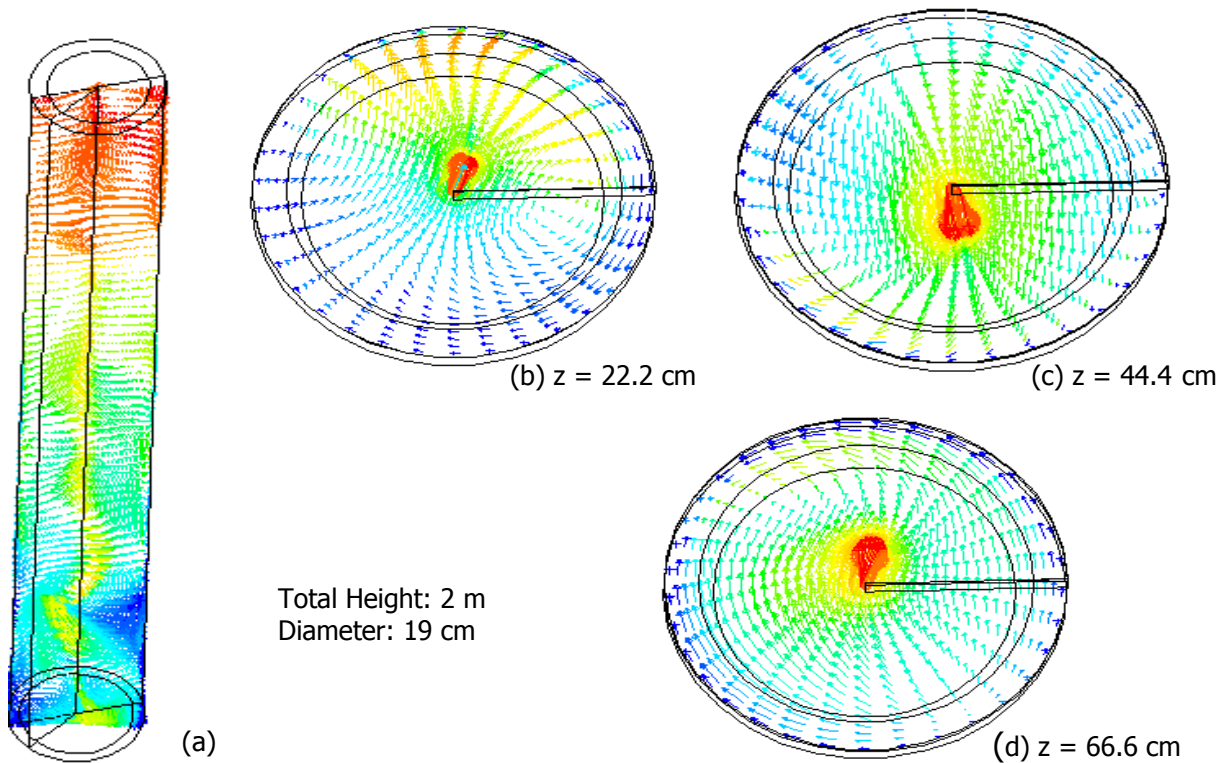


Figure 2.1 Instantaneous Velocity Vectors from Three-Dimensional Simulations ($U_g = 12$ cm/s)
(a) On a Single Vertical Plane; (b), (c), (d) At Three Horizontal Planes (Vectors are Colored by Gas Volume Fraction: Red = 0.8; Blue=0.1.) (Time = 10.04 s after $t = 0$.)

$z = 66.6 \text{ cm}$

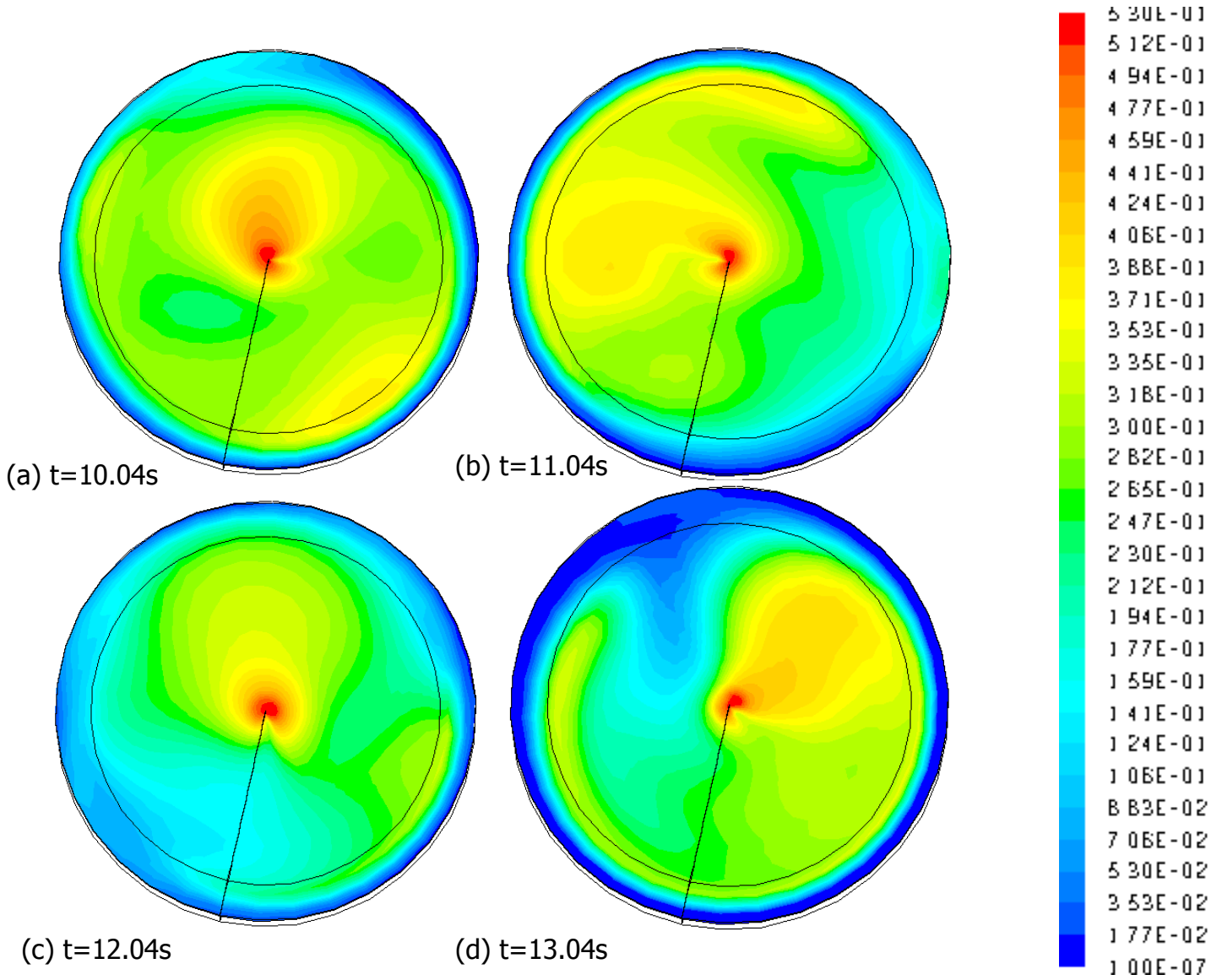


Figure 2.2 Instantaneous Gas Volume Fraction Contours from Three-Dimensional Simulations ($U_g = 12 \text{ cm/s}$) at Different Times at a Given Plane

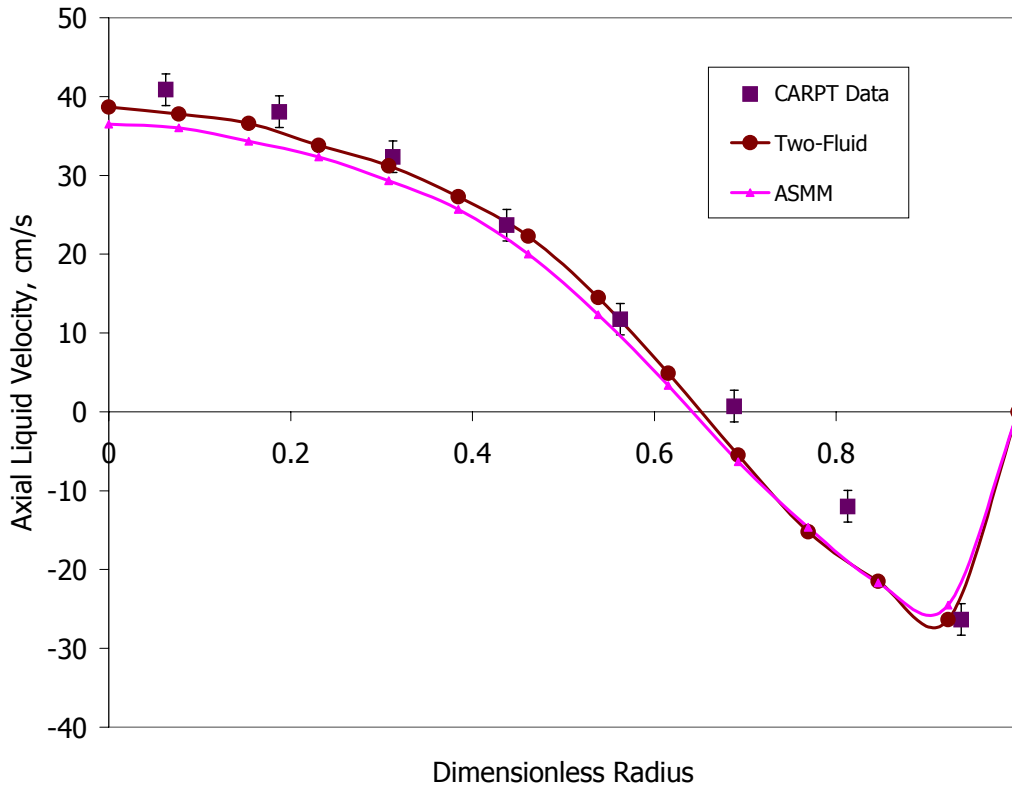


Figure 2.3 Time-Averaged Axial Liquid Velocity Profile ($U_g = 12$ cm/s)

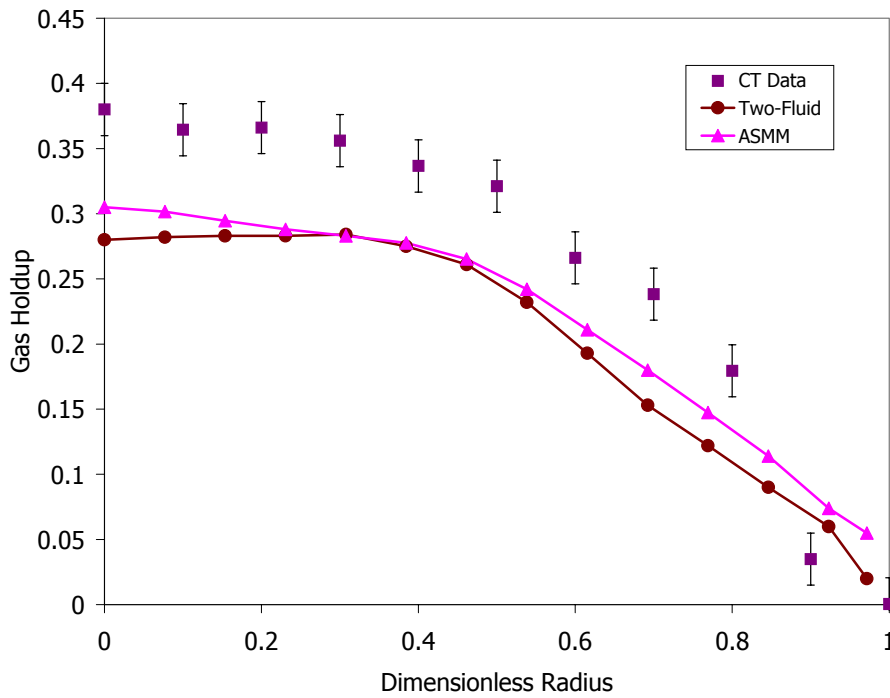


Figure 2.4 Time-Averaged Gas Volume Fraction Profile ($U_g = 12$ cm/s)

THE OHIO STATE UNIVERSITY

The report from Ohio State University for the period follows.

INTRINSIC FLOW BEHAVIOR IN A SLURRY BUBBLE COLUMN UNDER HIGH PRESSURE AND HIGH TEMPERATURE CONDITIONS

Quarter Report

(Reporting Period: April 1 to June 30, 1999)

Highlights

- The gas holdup in a high-pressure slurry bubble column was measured by the dynamic gas disengagement (DGD) technique. Examination of the effects of pressure and solids concentration on gas holdup revealed that elevated pressures lead to higher gas holdups in a slurry bubble column. The presence of particles reduced gas holdup at all pressures considered in this study.
- An empirical correlation was proposed to predict gas holdup in high-pressure slurry bubble columns of different scales. The correlation takes into account the experimental data obtained in this work, as well as the data in the literature for systems of various gas, liquid and solids mixtures.
- A similarity rule was revealed for the overall hydrodynamics of high-pressure slurry bubble columns. The rule takes into account the operating conditions, the maximum stable bubble size, and the physical properties of the gas, liquid and solids.
- The instantaneous flow fields during the DGD process were analyzed by using a PIV system to study the characteristics of bubble flow and to examine the assumptions used in existing DGD models.
- Experimental examinations of the roles of bubbles of different sizes indicated the importance of large bubbles in dictating the macroscopic hydrodynamics of slurry bubble columns because of their large volume, their high rise velocity, and the wakes associated with them.
- PIV measurement in the DGD process revealed that the existing DGD models can only provide preliminary estimations of the holdup structure and bubble size distribution in slurry bubble columns at low gas velocities. At high gas velocities, the bubble size

distribution cannot be reasonably estimated by the DGD technique without the quantification of bubble-bubble interactions. Direct measurement is the only accurate means to quantify bubble size distribution.

Work Conducted

Gas Holdup Correlation

Gas holdup is a key parameter in characterizing the macroscopic hydrodynamics of slurry bubble column systems. Gas holdup depends on gas and liquid velocities, gas distributor design, column geometry (diameter and height), physical properties of the gas and liquid, particle concentration, and physical properties of the particles. Gas holdup generally increases with an increase in gas velocity, and there is a greater increase in rate in the dispersed bubble regime than in the churn-turbulent regime. The distributor design significantly affects gas holdup only at low gas velocities. In bubble columns, the effect of column size on gas holdup is negligible when the column diameter is larger than 0.1 - 0.15 m (Shah et al., 1982). The influence of the column height is insignificant if the height is above 1 - 3 meters and the ratio of the column height to the diameter is larger than 5 (Kastaneck et al., 1984). The gas holdup decreases as liquid viscosity and/or gas-liquid surface tension increase; the effect of liquid density is not clear. The addition of particles into a bubble column leads to a larger bubble size and thus a decreased gas holdup, especially when the particle concentration is low. The particle size effect on gas holdup can be ignored in the particle size range of 44 - 254 μm . Detailed discussion of the dependence of gas holdup on various factors can be found in the reviews cited above.

Numerous studies have been conducted to investigate the effect of pressure on gas holdup in bubble columns (Tarmy et al., 1984; Idogawa, 1986; Wilkinson et al., 1992; Reilly et al., 1994; Jiang et al., 1995; Lin et al., 1998) and three-phase fluidized beds (Luo et al., 1997a). It is commonly accepted that elevated pressures lead to higher gas holdups in both bubble columns and three-phase fluidized beds except in those systems operated with porous plate distributors and at low gas velocities. The increased gas holdup is directly related to the smaller bubble size and, to a lesser extent, to the slower bubble rise velocity at higher pressures (Luo et al., 1997b). The most fundamental reason for the bubble size reduction is the variation in physical properties of the gas and liquid with pressure. Three mechanisms are involved: smaller initial bubble size from the gas distributor (larger gas density), reduced bubble coalescence rate (lower surface tension and higher liquid viscosity), and increased bubble breakup rate (higher gas density and lower surface tension). Empirical correlations have been proposed for the gas holdup in bubble columns operated at elevated pressure and temperature (Wilkinson et al., 1992; Reilly et al., 1994).

A significant pressure effect on gas holdup should exist in slurry bubble columns; however, little is reported concerning such an effect. Deckwer et al. (1980) found little effect of pressure on gas holdup in a Fischer-Tropsch slurry bubble column with a porous plate distributor ($P = 0.4 - 1.1 \text{ MPa}$; $T = 143 - 260^\circ\text{C}$; $U_g = 0 - 3.5 \text{ cm/s}$). The experimental data of Kojima et al. (1991) indicated that gas holdup increases with pressure; but no

pressure effect was observed at a 30 wt % solids concentration ($P = 0.1 - 1.1$ MPa; $U_g = 1.7 - 9$ cm/s; single orifice distributor). Inga (1997) measured gas holdup in slurry bubble columns for Fischer-Tropsch synthesis at pressures up to 0.72 MPa, and a significant pressure effect was observed. No viable model or correlation is available to predict the gas holdup in high-pressure slurry bubble columns. Thus, gas holdup behavior in high-pressure slurry bubble columns is not well understood, especially at high gas velocities.

A novel measuring technique, dynamic gas disengagement (DGD), was developed to measure gas holdup in a slurry bubble column under a wide range of operating conditions. This technique was detailed in a paper by Lee et al. (1998) and in previous monthly reports (April and May 1997). Experimental data on the effect of pressure on gas holdup were also provided in the previous monthly reports of December 1997 and January 1998. According to these data, elevated pressures lead to higher gas holdups in a slurry bubble column. The effect of solids concentration on overall gas holdup is shown in Figure 1. The presence of particles reduces gas holdup at both ambient and 5.6 MPa pressures, especially when the solids fraction is increased from 0 to 0.081. At ambient pressure, gas holdup in the bubble column ($\phi_s = 0$) is almost 100% higher than in the slurry of 0.191 solids volume fraction over the entire gas velocity range. In contrast, at a pressure of 5.6 MPa, the effect of solids concentration on gas holdup is relatively small at gas velocities above 25 cm/s. For example, at 5.6 MPa, gas holdup decreases from 0.55 to 0.48 (12%) as the solids fraction increases from 0 to 0.191 at a constant gas velocity of 30 cm/s; at ambient pressure the gas holdup decreases from 0.35 to 0.18 (49%) for the same solids concentration increase and at the same gas velocity.

Based on the experimental data in this work and on some available data in the literature, an empirical correlation (Eq. 1) is proposed to estimate the gas holdup in high-pressure slurry bubble columns:

$$\frac{\varepsilon_g}{1 - \varepsilon_g} = \frac{2.9 \left(\frac{U_g^4 \rho_g}{\sigma g} \right)^\alpha \left(\frac{\rho_g}{\rho_{sl}} \right)^\beta}{\left[\cosh(Mo_{sl}^{0.054}) \right]^{4.1}} \quad (1)$$

where Mo_{sl} is the modified Morton number for the slurry phase, $(\xi \mu_l)^4 g / \rho_{sl} \sigma^3$, and

$$\alpha = 0.21 Mo_{sl}^{0.0079} \quad \text{and} \quad \beta = 0.096 Mo_{sl}^{-0.011}.$$

The effective slurry density, ρ_{sl} , is given by

$$\rho_{sl} = \phi_s \rho_s + \phi_l \rho_l. \quad (2)$$

In Eq. (1), ξ is a correction factor that accounts for the effect of particles on slurry viscosity:

$$\ln \xi = 4.6\phi_s \left\{ 5.7\phi_s^{0.58} \sinh\left[-0.71 \exp(-5.8\phi_s) \ln(\text{Mo})^{0.22}\right] + 1 \right\}. \quad (3)$$

When the solids concentration approaches zero, this correlation reduces to the form for bubble columns.

The correlation takes into account not only the experimental data obtained in this work, but also the data obtained in systems of various gas, liquid, and solids by different authors. Table 1 lists the various experimental systems and their corresponding references. The average error of the predictions is 13% for both the slurry and gas-liquid systems, and the maximum error is 53%. Figure 2 shows the comparison between the predictions by the correlation and by the experimental data. The applicable ranges of the correlation are summarized in Table 2.

Similarity Rule

Based on the internal circulation model, which was presented in previous reports (January and February 1999), the maximum stable bubble size can be estimated by the following equations:

$$D_{\max} \approx 2.53 \sqrt{\frac{\sigma}{g\rho_g}} \quad (\text{bubble columns}) \quad (4a)$$

or

$$D_{\max} \approx 3.27 \sqrt{\frac{\sigma}{g\rho_g}} \quad (\text{slurry bubble columns}). \quad (4b)$$

The rise velocity of the maximum stable bubble, V_{\max} , can be estimated by

$$V_{\max} = \sqrt{\frac{2.8\sigma}{\rho_{sl}D_{\max}} + \frac{gD_{\max}}{2}} \approx 0.71\sqrt{gD_{\max}}. \quad (5)$$

Substituting Eq. (4a) into Eq. (5) yields

$$V_{\max} = 1.1g^{1/2} \left(\frac{\sigma}{g\rho_g} \right)^{1/4} \quad (6a)$$

or

$$V_{\max}^4 = 1.6g^2 \frac{\sigma}{g\rho_g} = \frac{1.6g\sigma}{\rho_g}. \quad (6b)$$

Thus, the dimensionless group of $U_g^4\rho_g / \sigma g$ in Eq. (1) can be rearranged to

$$\frac{U_g^4 \rho_g}{\sigma g} \propto \left(\frac{U_g}{V_{\max}} \right)^4. \quad (7)$$

Therefore, Eq. (1) can be rearranged to

$$\frac{\varepsilon_g}{1 - \varepsilon_g} \propto \frac{\left(U_g / V_{\max} \right)^{4\alpha} \left(\rho_g / \rho_{sl} \right)^\beta}{\cosh\left(\text{Mo}_{sl}^{0.054} \right)^{4.1}}. \quad (8)$$

Gas holdup is thus a function of a set of dimensionless groups, including U_g/V_{\max} , Mo_{sl} , and ρ_g/ρ_{sl} . It is clear that gas holdup behavior in high-pressure and high-temperature systems can be mimicked using low-pressure and low-temperature systems based on the matching of these dimensionless groups. As gas holdup is the principal variable that characterizes the hydrodynamic properties of bubble columns or slurry bubble columns, for high-pressure bubble columns and slurry bubble columns operated under a wide range of conditions, the hydrodynamic similarity requires these three dimensionless groups to be similar. To simulate the hydrodynamics of industrial reactors, cold models can be used and milder pressure and temperature conditions can be chosen, as long as the three groups are similar to those in the industrial reactor. The similarity rule needs to be tested in industrial reactors.

Flow Visualization of DGD Process

PIV Measurement in DGD Process

Dynamic gas disengagement experiments were conducted in a two-dimensional (2D) Plexiglas column under ambient conditions, as well as in a 3D column under high pressures. The instantaneous flow fields during the DGD process were analyzed using a PIV system to study the characteristics of bubble flow and to examine the assumptions used in the existing DGD models. The detailed experimental setup for the 2D column is provided by Lee et al. (1998). In the 2D column, the liquid phase used is tap water, and is operated under batch conditions with the static liquid height maintained near 120 cm. Compressed air and alumina particles of 100 μm mean diameter were used as the gas and solid phases, respectively. After steady-state operation was reached, the gas supply was shut off with a three-way valve, with one outlet being connected to the atmosphere, to prevent trickling bubbles from leaking into the column after shutoff.

The image of the flow field during the DGD process was recorded with a high framing-rate and high resolution CCD camera equipped with a variable electronic shutter ranging from 1/60 to 1/10,000 s. A framing rate of 240 fields/sec was used in this study. The images were analyzed using the PIV system originally developed by Chen and Fan (1992). This system was enhanced and modified to measure instantaneous full-field flow characteristics for a given plane. The modified PIV technique has sufficient accuracy to determine time/volume averaged flow information for each phase, including velocities and dispersed phase size distributions. Further, the PIV technique developed for multiphase systems can

discriminate between the different phases, and provides the instantaneous, full-field flow properties of each phase. With the PIV system, the transient flow behavior during the DGD process can be analyzed and compared to the assumptions made in various models.

Flow Characteristics from DGD Experiments

To fundamentally explain the effect of pressure on gas holdup in a slurry bubble column, it is essential to understand the flow characteristics and the bubble size variation with the pressure in the system. Frame-by-frame analysis of the instantaneous flow fields of the bubble phase reveals the importance of the interaction between small and large bubbles. A wake is formed when the bubble Reynolds number is above 20 for a single bubble (Fan and Tsuchiya, 1990). The wake behind the bubble generates a low-pressure region. Smaller bubbles are frequently attracted into the region and are accelerated to almost the same rise velocity as the leading bubble. This attraction phenomenon is evident in the results obtained from the DGD experiments. Figures 3(a) and 3(b) show the variations in the number of largest bubbles and the number of bubbles with the largest rise velocity during a DGD process. As the number of large bubbles gradually decreases during the DGD process, so does the rise velocity of the small bubbles. It is noted that bubbles larger than 2.0 cm rise at velocities of approximately 50 cm/s. The initial number of bubbles with a rise velocity higher than 50 cm/s is about 12, while the initial number of bubbles larger than 2.0 cm is only 2. Further, the number of fast-rising bubbles becomes zero only after the largest bubbles completely disengage at 1.5 s. The above observations clearly show the bubble wake attraction effect. Without such attraction, only the largest bubbles can reach this high velocity. Note that the superficial gas velocity in Figure 3 is 3.0 cm/s; as the superficial gas velocity increases, the effect of large bubbles on the rise velocity of the smaller bubbles becomes more dominant. Lee et al. (1998) studied the amount of small bubbles attracted by large bubbles with the PIV system in a 2D bubble column at various superficial gas velocities. They concluded that at gas velocities above 11 cm/s, over 70% of the initial small bubbles disengage from the column with the large bubbles; at gas velocities below 4 cm/s, the number is about 20%. The above observations undoubtedly indicate the dominant effect of large bubbles on the rise velocity of bubbles in bubble columns and slurry bubble columns. Moreover, the volume of a bubble is proportional to the cube of the bubble size. Since the gas holdup is basically dictated by the size and rise velocity of bubbles, the large bubbles play a key role in determining gas holdup in these systems.

The significance of the bubble wake attraction calls for examination of the existing models that describe the DGD profiles, i.e., the gas holdup or liquid height variation with time during the DGD process. The various existing DGD models are summarized in Figure 4, in which the gas is shut off at t_0 . If a bimodal bubble size distribution is assumed, the DGD profile can be approximated by two straight lines. The line with a steeper slope corresponds to the escape of both large and small bubbles in stage one; the other line corresponds to the escape of the small bubbles in stage two. If the rise velocity of the small bubbles is assumed to be constant throughout the entire disengagement process, the line for stage two can be extrapolated to t_0 to obtain the initial holdup of the small bubbles (Sriram and Mann, 1977), marked as Model 1 in Figure 4. If it is assumed that the small

bubbles do not disengage in stage one due to the liquid backflow (Model 2), the initial small bubble holdup is simply the gas holdup at t_1 , i.e., at the end of stage one (Vermeer and Krishna, 1981). The other assumption regarding the disengagement rate of bubbles is that the slip velocity between the gas and the liquid is constant (Patel et al., 1989). In this case, the calculated small-bubble holdup falls between the values of Model 1 and Model 2. However, since all three assumptions regarding the small bubble rise velocity do not recognize the bubble acceleration due to the large bubbles at the first stage, the models may lead to errors in estimating holdups for both small and large bubbles, especially at high superficial gas velocities, as shown in Figure 4. The above analysis is based on a bimodal bubble size assumption; the true bubble disengagement behavior is even more complex, as the bubble size distribution is known to be continuous. The liquid circulation in the column further complicates the analysis of the DGD processes (Desphande et al., 1995).

In addition to the bubble wake attraction, strong bubble coalescence and breakup are also observed during the DGD process, which invalidates the first assumption made in the existing DGD models, i.e., no bubble coalescence and breakup. However, the error due to this assumption is minimal if a dynamic equilibrium between the bubble coalescence and the bubble breakup can be assumed.

In summary, the intrinsic bubble flow behavior in the dynamic gas disengagement process is complex in nature. Through the bubble wake attraction, the gas holdups in bubble columns or slurry bubble columns are closely associated with the size and number of large bubbles. A fundamental explanation of the pressure effect on gas holdup should be based on a full understanding of the variation in bubble size, especially of large bubble size, with pressure. The existing DGD models can only provide preliminary estimations of the holdup structure and bubble size distribution in slurry bubble columns at low gas velocities. In slurry bubble column reactors operated at high gas velocities, such as those in the methanol synthesis process, the bubble size distribution cannot be reasonably estimated by the DGD technique without the quantification of bubble-bubble interactions. Therefore, direct measurement is the only accurate means to quantify bubble size distribution.

Notations

d_b	bubble size
D_c	column diameter
D_{\max}	maximum stable bubble size
d_p	particle size
g	gravitational acceleration
H	column height
Mo	Morton number
P	pressure
T	temperature
t	time
U_b	bubble rise velocity
U_g	superficial gas velocity
V_{\max}	rise velocity of maximum stable bubble

Greek letters

σ	surface tension
ε	phase holdup
ϕ	volume fractions of liquid or solids in a slurry
μ	viscosity
ρ	density
ξ	parameter accounting for the effect of particles on the viscosity

Subscripts

g	gas phase
l	liquid phase
s	solids phase
sl	suspension

References

- Akita, K., and F. Yoshida, "Gas Holdup and Volumetric Mass Transfer Coefficient in Bubble Columns," *Ind. Eng. Chem. Process Des. Develop.*, **12**, 76 (1973).
- Bach, H. F., and T. Pilhofer, "Variation of Gas Hold-Up in Bubble Columns with Physical Properties of Liquids and Operating Parameters of Columns," *Ger. Chem. Eng.*, **1**, 270 (1978).
- Chen, R. C. and L. S. Fan, "Particle Image Velocimetry for Characterizing the Flow Structure in Three-Dimensional Gas-Liquid-Solid Fluidized Beds," *Chem. Eng. Sci.*, **47**, 3615 (1992).
- Deckwer, W. D., Y. Louisi, A. Zaidi, and M. Ralek, "Hydrodynamic Properties of the Fischer-Tropsch Slurry Process," *Ind. Eng. Chem. Proc. Des. Dev.* **19**, 699 (1980).
- Desphande, N. S., M. Dinkar, and J. B. Joshi, "Disengagement of the Gas Phase in Bubble Columns," *Int. J. Multiphase Flow*, **21**, 1191 (1995).
- Fan, L. S. and K. Tsuchiya, *Bubble Wake Dynamics in Liquids and Liquid-Solid Suspensions*, Butterworth-Heinemann, Stoneham, MA (1990).
- Idogawa, K., K. Ikeda, T. Fukuda, and S. Morooka, "Behavior of Bubbles of the Air-Water System in a Column under High Pressure," *Int. Chem. Eng.*, **26**, 468 (1986).
- Inga, J. R., *Scaleup and Scaledown of Slurry Reactors: A New Methodology*, Ph.D. thesis, University of Pittsburgh, USA (1997).
- Jiang P., T. J. Lin, X. Luo, and L. S. Fan, "Visualization of High Pressure (21 MPa) Bubble Column: Bubble Characteristics," *Chem. Eng. Res. & Des.*, **73**, 269 (1995).
- Kastaneck, F., J. Zahradnik, J. Kratochvil, and J. Cermak, "Modelling of Large-Scale Bubble Column Reactors for Non-Ideal Gas-Liquid Systems," in *Frontiers in Chemical Reaction Engineering*, ed. by Doraiswamy, L.K. and R. A. Mashelkar, **1**, 330, Wiley, Bombay, India (1984).
- Koide, K., A. Takazawa, and M. Komura, "Gas Holdup and Volumetric Liquid-Phase Mass Transfer Coefficient in Solid-Suspended Bubble Columns," *J. Chem. Eng. Japan*, **17**, 459 (1984).
- Kojima, H., B. Okumura, and A. Nakamura, "Effect of Pressure on Gas Holdup in a Bubble Column and a Slurry Bubble Column," *J. Chem. Eng. Japan*, **24**, 115 (1991).
- Krishna, R., P. M. Wilkinson, and L. L. van Dierendonck, "A Model for Gas Holdup in Bubble Columns Incorporating the Influence of Gas Density on Flow Regime Transitions," *Chem. Eng. Sci.*, **46**, 2491 (1991).
- Lee, D. J., X. Luo, and L. S. Fan, "Gas Disengagement Technique in a Slurry Bubble Column Operated in the Coalesced Bubble Regime," paper P-14 presented at the 15th International Symposium of Chemical Reaction Engineering, Newport Beach, California, September 13-16 (1998).
- Li, H., and A. Prakash, "Heat Transfer and Hydrodynamics in a Three-Phase Slurry Bubble Column," *Ind. Eng. Chem. Res.*, **36**, 4688 (1997).
- Lin, T. J., K. Tsuchiya, and L. S. Fan, "Bubble Flow Characteristics in Bubble Columns at Elevated Pressure and Temperature," *AIChE J.* **44**, 545 (1998).
- Luo, X., J. Zhang, K. Tsuchiya, and L. S. Fan, "On the Rise Velocity of Bubbles in Liquid-Solid Suspensions at Elevated Pressure and Temperature," *Chem. Eng. Sci.*, **52**, 3693 (1997b).

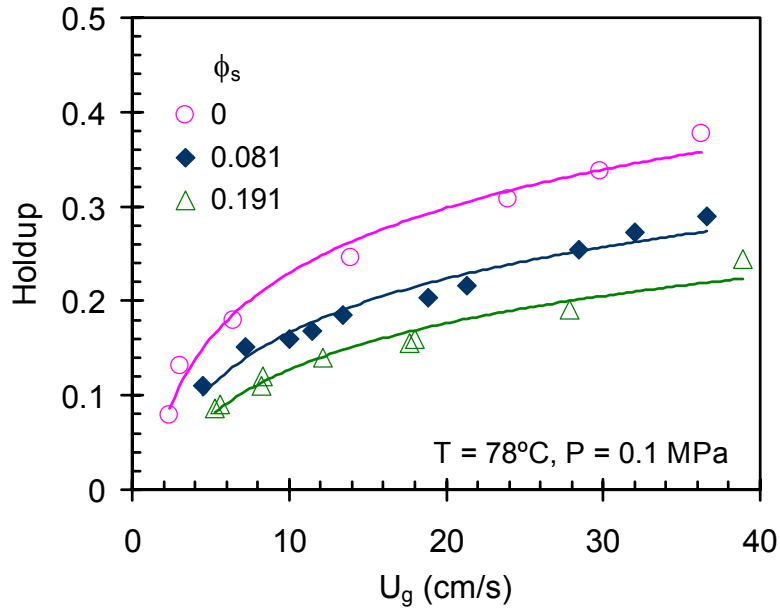
- Luo, X., P. Jiang, and L. S. Fan, "High Pressure Three-Phase Fluidization: Hydrodynamics and Heat Transfer," *AIChE J.*, **43**, 2432 (1997a).
- O'Dowd, W., D. N. Smith, J. A. Ruether, and S. C. Saxena, "Gas and Solids Behavior in a Baffled and Unbaffled Slurry Bubble Column," *AIChE J.*, **33**, 1959 (1987).
- Oyevaar, M., *Gas-Liquid Contacting at Elevated Pressures*, Ph.D. thesis, Twente University, The Netherlands (1989).
- Patel, S. A., J. Daly, and D. Bukur, "Holdup and Interfacial Area Measurements Using Dynamic Gas Disengagement," *AIChE J.*, **35**, 931 (1989).
- Petukhov, V. I., and V. A. Kolokol'tsev, "Effect of Liquid Viscosity on Droplet Entrainment and Volumetric Air Content," *Therm. Eng.*, **12**, 41 (1965).
- Reilly, I. G., D. S. Scott, T. J. W. de Bruijn, and D. MacIntyre, "The Role of Gas Phase Momentum in Determining Gas Holdup and Hydrodynamic Flow Regimes in Bubble Column Operations," *Can. J. Chem. Eng.*, **72**, 3 (1994).
- Saxena, S. C., R. Vadivel, and A. C. Saxena, "Gas Holdup and Heat Transfer from Immersed Surfaces in Two- and Three-Phase Systems in Bubble Columns," *Chem. Eng. Comm.*, **85**, 63 (1989).
- Shah, Y. T., B. G. Kelkar, S. P. Godbole, and W. D. Deckwer, "Design Parameters Estimations for Bubble Column Reactors," *AIChE J.*, **28**, 353 (1982).
- Shollenberger, K. A., and T. J. O'Hern, "Characterization of Slurry-Phase Flow in the LaPorte Alternative Fuels Development Unit (AFDU) Using Differential Pressure Measurements," U.S. DOE Report, under contract number DE-FC22-95 PC 95051 (1997).
- Sriram, K., and R. Mann, "Dynamic Gas Disengagement: A New Technique For Assessing the Behaviour of Bubble Columns," *Chem. Eng. Sci.*, **32**, 571 (1977).
- Tarmy, B., M. Chang, C. Coualoglou, and P. Ponzi, "Hydrodynamic Characteristics of Three Phase Reactors," *The Chemical Engineer*, **407**, 18 (1984).
- Vermeer, D. J. and R. Krishna, "Hydrodynamics and Mass Transfer in Bubble Columns Operating in the Churn-Turbulent Regime," *Ind. Eng. Chem. Process Des. Dev.*, **20**, 475 (1981).
- Wilkinson, P. M., A. P. Sper, and L. L. van Dierendonck, "Design Parameters Estimation for Scaleup of High-Pressure Bubble Columns," *AIChE J.*, **38**, 544 (1992).

Table 1 List of the Various Experimental Systems and References Selected

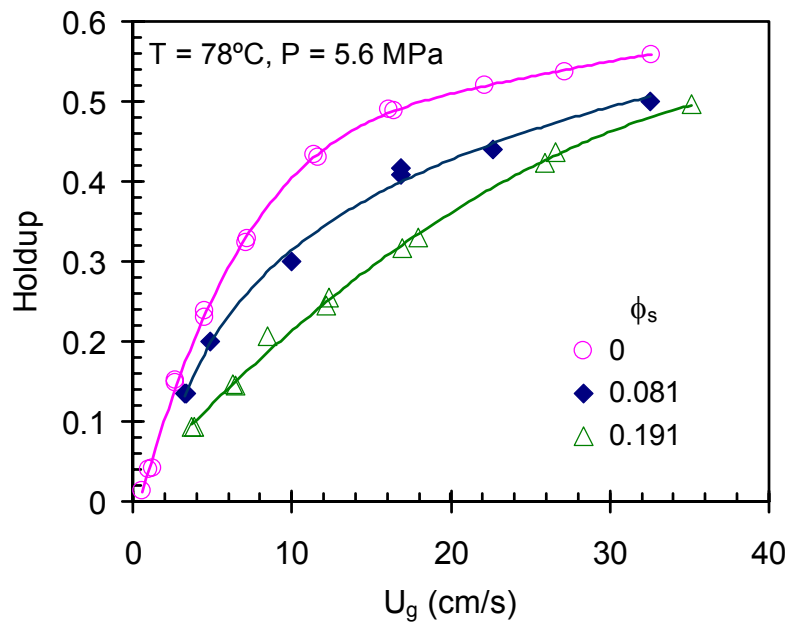
GAS/LIQUID/SOLIDS SYSTEMS	REFERENCES	SYMBOLS IN FIG. 2
Air/methanol, air/water, air/glycol, He/water, CO ₂ /water	Akita and Yoshida (1973)	—
Air/tetrabromoethane, air/n-octanol, air/ethylene glycol, air/butan-diol(1,3)	Bach and Pilhofer (1978)	-
CH ₄ /C ₆ /FeOx, CO/C ₆ /FeOx, N ₂ /C ₆ /FeOx, H ₂ /C ₆ /FeOx	Inga (1997)	□
Air/water, air/water/glass beads	Koide et al. (1984)	+
Ar/water, N ₂ /water, N ₂ /turpentine, N ₂ /butanol, N ₂ /MEG	Krishna et al. (1991)	▲
Air/water/glass beads	Li and Prakash (1997)	◇
N ₂ /water/glass beads	O'Dowd et al. (1987) Saxena et al. (1989)	□
N ₂ /water	Oyevaar (1989)	■
N ₂ /water	Petukhov and Kolokol'tsev (1965)	△
Air/Isopar G, He/water, air/water, air/trichloroethylene	Reilly et al. (1994)	×
N ₂ /Drakeol-10/ZnO _x , N ₂ /Drakeol-10/CuO _x , N ₂ /Drakeol-10/Alumina	Shollenberger et al. (1997)	△
N ₂ /n-heptane	Tarmy et al. (1984)	◆
N ₂ /n-heptane, N ₂ /MEG, N ₂ /water	Wilkinson et al. (1992)	○

Table 2 Applicable Range of the Gas Holdup Correlation

PARAMETER (UNITS)	RANGE
ρ_l (kg/m ³)	668 – 2965
μ_l (mPa-s)	0.29 – 30
σ_l (N/m)	0.019 - 0.073
ρ_g (kg/m ³)	0.2 – 90
ϕ_s (-)	0 - 0.4
D_p (μm)	20 – 143
ρ_s (kg/m ³)	2200 – 5730
U_g (m/s)	0.05 - 0.69
U_l (m/s)	0 (batch liquid)
D_c (m)	0.1 - 0.61
H/D_c (-)	> 5
Distributor types	Perforated plate, sparger, and bubble cap



(a)



(b)

Figure 1 Effect of Solids Concentration on Gas Holdup at Two Pressures: (a) $P = 0.1$ MPa; (b) $P = 5.6$ MPa

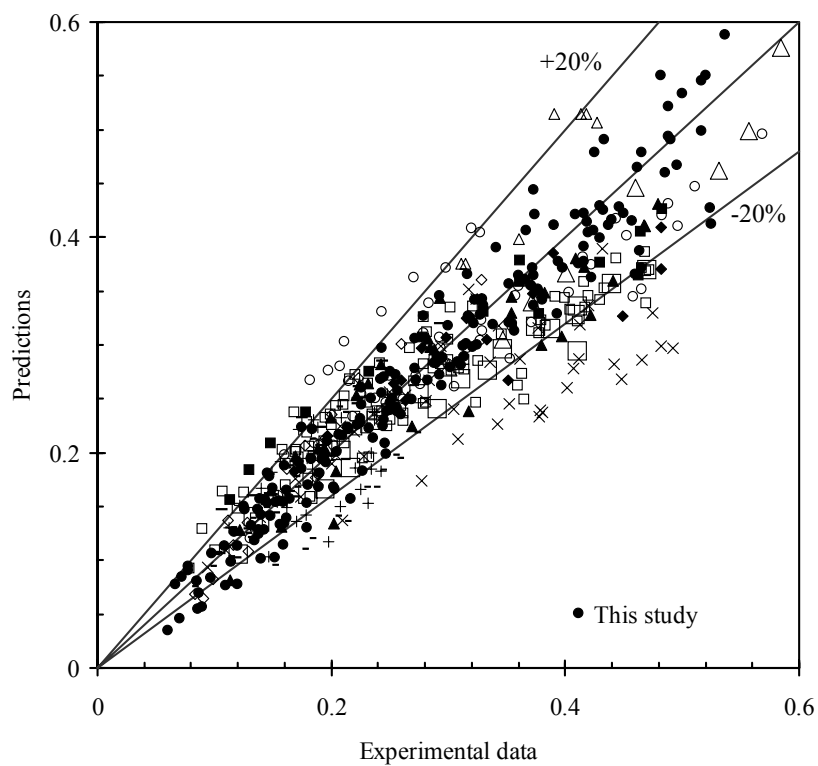
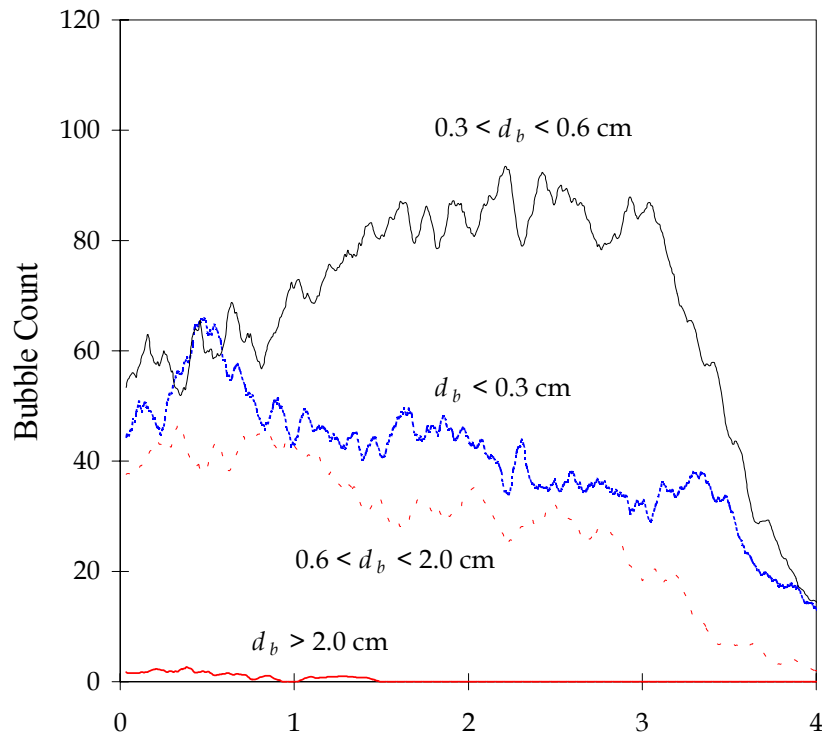
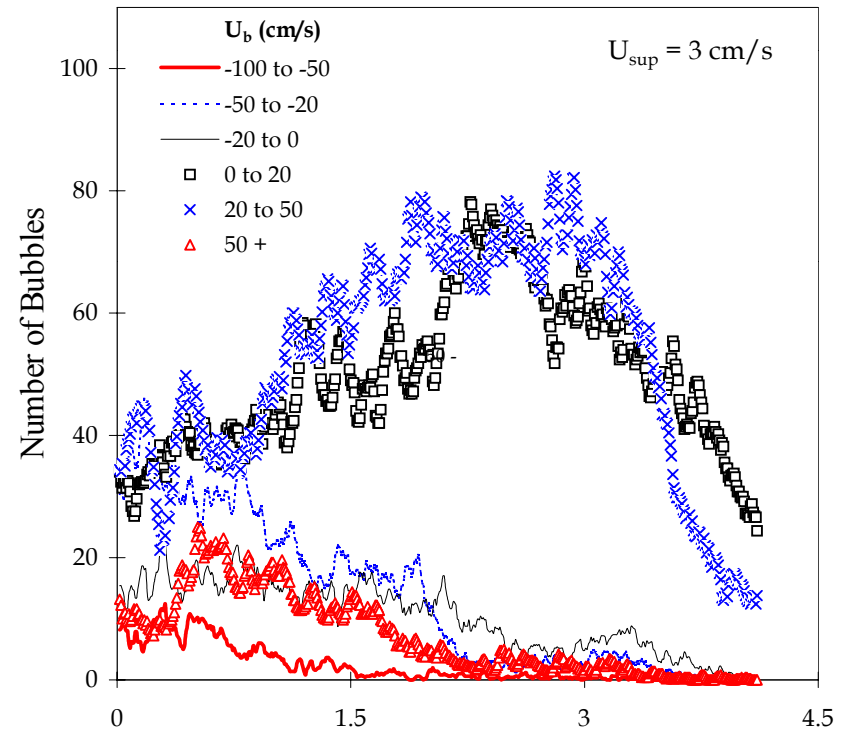


Figure 2 Comparison between the Predicted Gas Holdup and the Experimental Data (For symbols of literature data, see Table 1.)



(a)



(b)

Figure 3 Bubble Flow Characteristics during a DGD Process: (a) bubble size variation ($U_g = 3.0$ cm/s, from Lee et al., 1998); (b) bubble rise velocity variation

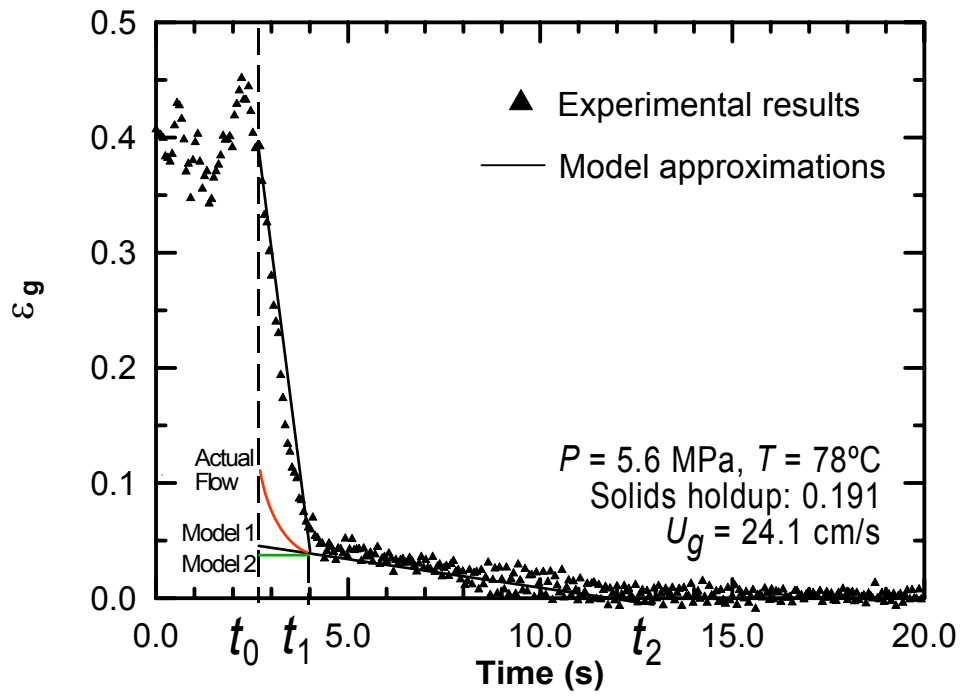


Figure 4 Characteristics of Models 1, 2 in Accounting for the Experimental Gas Holdup Variation during the Gas Disengagement Process